Solar Activity Cycle: History and Predictions

George L. Withbroe*
Harvard-Smithsonian Center for Astrophysics, Cambridge, Massachusetts

The solar output of short-wavelength radiation, solar wind, and energetic particles depends strongly on the solar cycle. These energy outputs from the sun control conditions in the interplanetary medium and in the terrestrial magnetosphere and upper atmosphere. Consequently, there is substantial interest in the behavior of the solar cycle and its effects. This review briefly discusses historical data on the solar cycle and methods for predicting its future behavior, particularly for the current cycle, which shows signs that it will have moderate to exceptionally high levels of activity. During the next few years, we can expect that the solar flux of short-wavelength radiation and particles will be more intense than normal and that spacecraft in low Earth orbit will re-enter earlier than usual.

Introduction

THE sun is a remarkable object. Nearly all of its energy emerges in the form of low-energy photons in the ultraviolet through infared regions of the spectrum. At these wavelengths, the solar output is nearly constant, varying only a fraction of a percent. This near constancy of the low-energy solar output provides the Earth with the steady source of radiative input required to create the stable weather conditions that have permitted terrestrial life to flourish. However, at higher energies, in the extreme ultraviolet, x-ray, and gamma-ray wavelengths, the solar radiative output is highly variable. This is illustrated in Fig. 1. Figure 1a shows the solar variability in 1979 at various ultraviolet and extreme ultraviolet (EUV) wavelengths between 28.4 and 205 nm (284–2050 Å).[1] Figure 1b shows the solar uv spectrum (top) and an estimate of the spectral variability during cycle 21 (bottom). The solar output of particles also exhibits strong variations. It consists of both low-energy particles forming the solar wind, which has a mean outflow speed of about 400 km/s, and high-energy particles (electrons, protons, and heavier ions), which move at near light speeds. The variable component of the solar output has a cyclic behavior which rises and falls with a period of about 11 yr. This review briefly discusses historical data on the solar cycle and methods for predicting its future behavior. The discussion of predictions is limited to consideration of long-term solar variations (months, years) and does not consider an equally important topic, the prediction of short-term (minutes, hours) behavior of solar activity.

Discovery of the Solar Cycle

The solar cycle was discovered by Schwabe[2] in 1843 from observations of sunspots, which are small dark areas on the solar surface. He noted that the number of sunspots on the sun varied with a period of about 10 yr. His discovery was made possible by Galileo's finding that sunspots could be observed with the recently invented telescope. In 1848, Wolf began tabulating the daily number of sunspots using as an index a number that depends on the number of spots and spot groups on the sun: the Wolf sunspot number $R = k(10g + f)$.[3] The factor k depends on the "seeing" or quality of the observing conditions due to fluctuations in the Earth's atmosphere (which affects the visibility of small sunspots), the "personal equation" of the observer, and the type of measurement (instrument used; visual or photographic observations). The parameters g and f are, respectively, the number of sunspot groups (clusters of sunspots) and the number of individual spots. Hence, the sunspot number is not a true measurement, but a semiquantitative indicator of "spotiness." In spite of this deficiency, it has proven to be a good index for determining how active the sun is.

Figure 2 shows the annual mean sunspot numbers from 1610 (when the telescope was invented) until 1975. As is readily apparent, the sunspot cycle is irregular. The most prominent features are its appoximatley 11-yr period, the variation of the magnitude of sunspot number at maximum, and the long period of very low sunspot numbers in the last half of the seventeenth century. The latter period is known as the Maunder minimum.[4] The most reliable data are those from about 1850.[4] Since then, the period of the sunspot cycle has been as short as 10.0 yr and as long as 12.1 yr, with the mean period being about 11 yr.[5] The average time from minimum to maximum is 4.3 yr, and the average time from maximum to minimum is 6.6 yr. Cycles with faster rise times typically have higher maxima.[5,6] The mean height of the sunspot maximum is $R_{max} = 116$ (for last 12 cycles R).[6] The largest maximum was observed during the 1957–1958 maximum (designated solar cycle 19) when the smoothed sunspot number reached a value of 201. Because of the large fluctuations in the short-term (days to months) sunspot numbers, smoothed numbers are usually used, with a 12- or 13-month running mean being a typical measure of spotiness.

With the advent of more modern techniques for observing the sun, there are now other solar indices that provide better quantitative measurements of solar activity. The most widely used of these is the solar 10.7-cm radio flux, the brightness of the sun as observed at a wavelength of 10.7 cm. The solar 10.7-cm flux, which has been measured regularly since 1947, has provided a reliable, quantitative measure of solar activity over the past four solar cycles. Surprisingly (give the qualitative nature of the sunspot number), there is a strong correlation between the sunspot number and the 10.7-cm flux. This is illustrated in Fig. 3. The relationship between these two indices is $R = 1.075F_{10.7} - 61.1$, when 13-month means are used.[6] The 10.7-cm flux is also strongly correlated with the solar EUV flux which plays a primary role in heating the outer atmosphere of the Earth (see Fig. 1; review by Hedin and Mayr[7]). Because measurements of the 10.7-cm flux have been available throughout the space age, while measurements of the EUV flux have been made over only relatively short intervals, the 10.7-cm flux is usually taken as a proxy for the EUV flux and is frequently used in calculational models for the upper terrestrial atmosphere.[7] The daily fluctuations in the 10.7-cm

Received Dec. 6, 1988; presented as at the AIAA Aerospace Engineering Conference and Show, Los Angeles, CA, Feb. 14–16, 1989; revision received March 20, 1989.

*Associate Director, Solar and Stellar Physics Division.

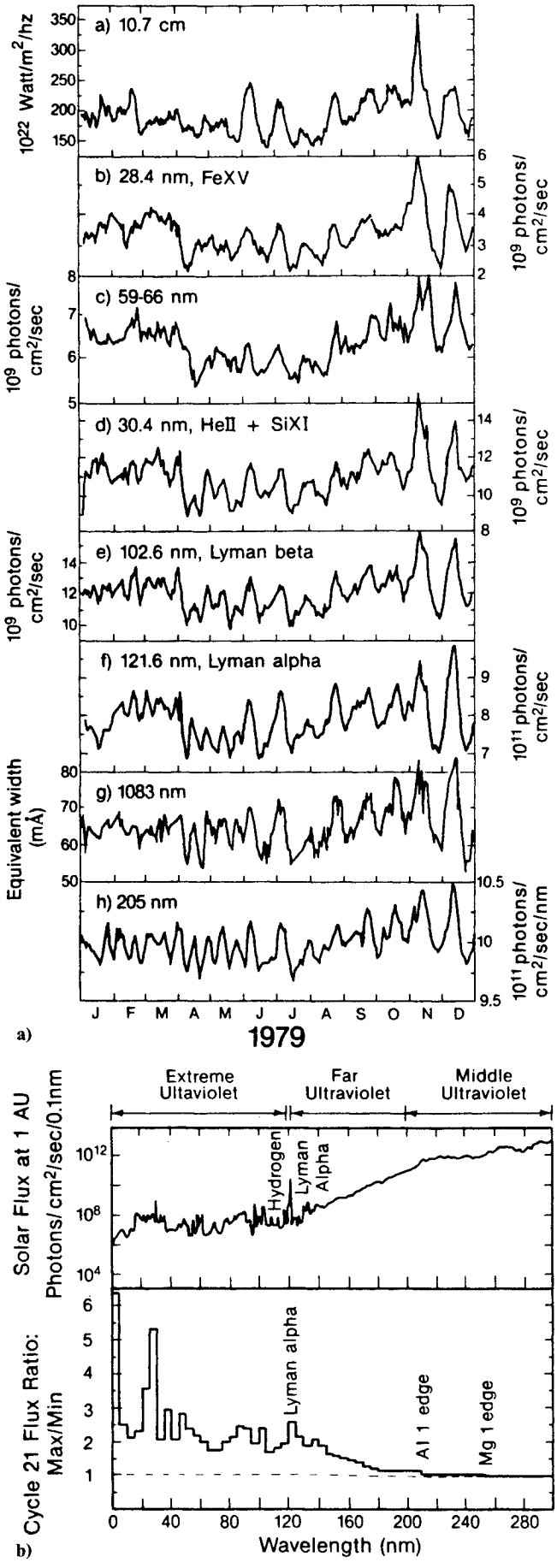

Fig. 1 a) Solar variability in 1979 at several radio, uv and EUV wavelenths;[1] b) The solar uv spectrum (top) and an estimate of the spectral variability during cycle 21 (bottom).

flux (and in the sunspot number) can be large, as illustrated in Fig. 4, which compares daily measurements with the smoothed (13-month running mean) values from cycle 19.

Sunspots and other direct indicators of solar activity have been observed for a relatively short interval of time. One method of extending our knowledge of solar activity to earlier times is through use of secondary measures of solar activity. One of these proxies is the amount of radiocarbon ^{14}C in tree rings.[8] Radiocarbon is produced by interactions of high-energy cosmic rays with the terrestrial atmosphere. Since the cosmic ray flux in the solar system is modulated by solar activity, measurements of the amount of ^{14}C as a function of time can provide a record of solar activity. As indicated by Eddy,[8] use of radiocarbon measurements in tree rings to infer the level of solar activity has limitations, because the filtering caused by varying patterns of atmospheric circulation, diffusion, and ocean absorption delay and dilute real variations in the radiocarbon production, and severely attenuate changes shorter than about 20 yr. Thus, only long-term, gross effects can be observed. These are illustrated in Fig. 5. The upper graph gives the persistent radiocarbon deviations. Downward excursions indicate increased ^{14}C and imply decreased solar activity. The circled numbers indicate significant minima and maxima including the Maunder minimum (2). The middle curve is a interpretation of the radiocarbon record as being an envelope of solar activity. Note that the period of time, 1600 to the present, corresponds to the time interval given in Fig. 2 for the sunspot data. The left-hand bottom curve gives the times of advance and retreat of Alpine glaciers. The dashed curve gives the mean annual temperature in England, and the solid curve in the lower right gives the winter-severity index (colder downward) for the Paris–London area. Note that there appear to be several periods in the past when the sun may have been more active that during the present era (e.g., maxima labeled 12, 11, 10, 6, and 4).

Solar Magnetic Cycle

The sunspot cycle is one manifestation of a more basic solar cycle, the solar magnetic cycle. Babcock's model provides a simple qualitative explanation for many of the observed properties of the sunspot cycle.[9,10] Among the features of the sun-spot cycle to be explained are as follows:

1) The first spots observed in a cycle appear at high latitudes ($\sim 30°$).

2) As the cycle progresses, new spots are born at progressively lower latitudes, until near the end of the cycle they form close to the equator.

3) Sunspots are regions with strong magnetic fields. These strong fields produce sunspots by inhibiting the outward convective flow of energy from the solar interior to form relatively cool areas (hence dark spots) at the surface.

4) Sunspots appear in groups with the leader spots (in that they lead the way across the disk as the sun rotates) in the one hemisphere (e.g., northern hemisphere) having positive polarity, while the follower spots have negative polarity. In the other hemisphere (e.g., southern), the leader and follower spots have the opposite polarities (leading spots negative, following spots positive).

5) In the next cycle the polarities are reversed in the two hemispheres.

In Babcock's model, the sunspot cycle is caused by the interaction between the sun's rotation and its magnetic field.[9,10] The sun rotates differentially; that is, the rotation rate is highest at the equator and decreases with increasing solar latitude such that the rotation rate at the poles is about 20% slower than at the equator. As viewed from the Earth, the equatorial rotation rate is about 27 days. At the start of the 11-yr solar cycle, the configuration of the solar magnetic field is similar to the Earth's, with positive polarity at the north pole of the sun and negative polarity at the south (see Fig. 6). The magnetic field lines run primarily from north to south.

Then differential rotation begins to stretch the field lines as more rapidly rotating equatorial regions run ahead of the regions at higher latitudes. The stretched field lines below the solar surface become twisted and intensified until bundles of twisted field lines become buoyant and pop through the surface forming magnetic bipolar regions. Polarity is positive where one end of each flux bundle passes through the surface and negative at the other end. Motions of the gas at the solar surface cause the surface fields to break up with the following polarities drifting toward the poles where they mix with the opposite polarities there. This cancels existing polar fields and eventually replaces them with fields of the opposite polarity. Eventually (after about 11 yr), the global field reverses, forming a situation similar to that at the start, but with opposite polarities at the solar poles (negative polarity at the north pole, positive polarity at the south pole). This sets the stage for a similar cycle of winding up of the fields, etc. Thus, the 22-yr magnetic cycle has two maximum periods of strong magnetic fields at the surface, periods when there are many sunspots and extensive amounts of solar activity.

The magnetic fields that reach the solar surface produce other structures besides sunspots. Magnetic loops extend above the surface connecting regions of opposite magnetic polarity and become filled with hot plasma with temperatures of 1.5 to 3×10^6 K. The plasma heating appears to be caused by quasisteady-state dissipation of magnetic energy stored in the twisted magnetic-field lines. This region of the solar atmosphere is known as the corona. It emits EUV and x-ray radiation, which can be observed with instruments flown above the EUV/x-ray absorbing layers of the Earth's upper atmosphere. Figure 7 shows a map of the positive and negative magnetic polarities at the solar surface as light and dark areas (lower right photograph). The other three photographs show the coronal loops as observed in EUV emissions at wavelengths corresponding to highly ionized atoms which map the plasma at mean temperatures of 6×10^5 K (Ne VII line at 465 Å), 10^6 K (Mg IX line at 368 Å), and 2.5×10^6 K (Fe XV line at 284 Å). Ne VII is a neon atom with 6 electrons removed. Since the amount of EUV and x-ray radiation emitted by the sun depends on the fraction of the solar surface covered by strong magnetic fields, the EUV and x-ray energy received by the Earth depends on solar rotation (since the magnetic fields are not uniformly distributed) and upon the solar cycle.

In some areas of the sun, the magnetic fields are sufficiently weak that the gas pressure of the hot coronal plasma exceeds the pressure of the magnetic field, breaking open the magnetic loops, and allowing the plasma to flow out into interplanetary space to form the solar wind.[11-13] The most prominent sources of steady-state solar wind are coronal holes, large magnetic unipolar regions with open magnetic configurations (one end of each field line is rooted in the sun, the other is carried far out into space by the solar wind). The large dark areas in the x-ray photograph of the sun (Fig. 8) are coronal holes. The bright areas are regions with closed magnetic-field configurations (magnetic loops with both ends of the field lines attached to the solar surface). Regions with the strongest magnetic fields have the brightest x-ray emission. Coronal holes are sources of highspeed solar wind (mean speed of about 700 km/s).[14-17] Small open areas within magnetically complex regions appear to be the source of the low-speed wind[18] (mean speed of about 340 km/s). Magnetically complex regions appear to have predominantly closed configurations and are characterized by moderate to bright x-ray emissions (see Fig. 8).

Occasionally, energy stored in the twisted magnetic-field lines is released suddenly. This sudden energy release accelerates electrons, protons, and ions to high energies and heats the solar gas to high temperatures, typically several times 10^7 K. This is a solar flare.[19-21] The high-temperature gas generates intense bursts of x-ray and EUV radiation, which travel outward into interplanetary space at the speed of light and, among other things, heat and ionize gas in the upper terrestrial

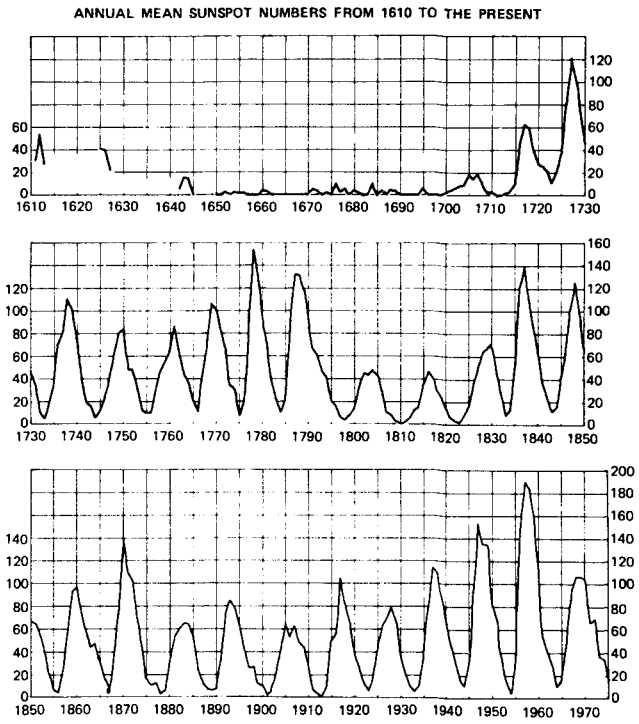

Fig. 2 Annual mean sunspot numbers from 1610–1975.[4]

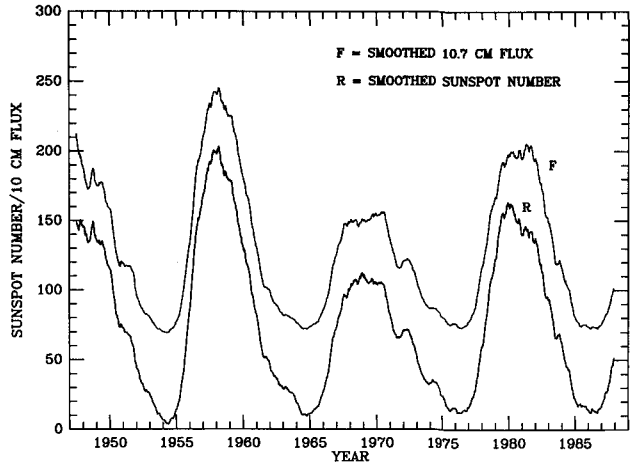

Fig. 3 Smoothed (13-month running mean) sunspot number *R* and solar 10.7-cm radio flux *F*.

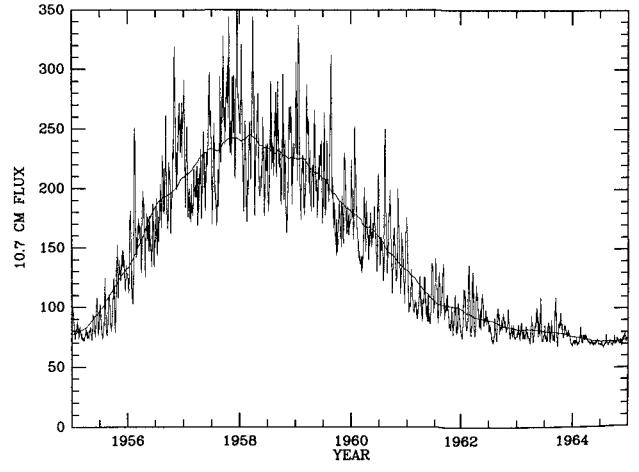

Fig. 4 Smoothed and daily 10.7-cm flux for cycle 19.

atmosphere. Some of the high-energy accelerated particles may also escape the sun and if conditions are suitable, some of these particles may reach the Earth. (Flares that occur near the west limb of the sun tend to have more favorable conditions for this due to the configuration of the interplanetary magnetic field, which spirals out from the rotating sun much like the water from a rotating water sprinkler. The solar magnetic-field lines are carried away from the sun by the solar wind.) Finally, the disruption of the coronal magnetic field may also blow off large amounts of coronal gas, which produces what is known as a coronal mass ejection.[22,23] If this plasma cloud (enhanced solar wind) is directed toward the Earth and impacts on the Earth's magnetosphere, it affects conditions in the magnetosphere and upper atmosphere.[24] Figure 9 contains a photograph of a coronal mass ejection (large bright feature on left) observed during its passage through the outer corona. The other bright, nearly radial, features are streamers (e.g., features on the right) which overlie large-scale magnetic bipolar regions. This photograph was acquired by the Skylab white-light coronagraph which had an occulting disk which blocked the solar emission out to 1.5 solar radii from suncenter.

Figure 10 illustrates how the number of flares varied during the last solar cycle.[5] Optical flares are flares that are observed in visible light with a telescope that has a filter which permits observation of the chromosphere via emission from the hydrogen Hα line at 6563 Å. The chromosphere is a thin layer of the solar atmosphere between the visible surface of the sun (photosphere) and the hot corona. Most flares do not emit measurable amounts of white-light radiation; they are best observed in emissions from the chromosphere or corona. As indicated earlier, flares emit strong x-ray emission. Figure 10 shows the number of class X flares (large x-ray fluxes) and the number of class M flares (moderate x-ray fluxes). The figure also gives the number of high-energy proton events (proton flux at the Earth ≥ 10 cm-2s^{-2}sr^{-1} for protons with energy ≥ 10 MeV).

The remaining graph in Fig. 10 gives the number of geomagnetic storms as a function of time in cycle 21. These are usually caused by high-speed solar wind streams generated by coronal mass ejections and by coronal holes.[25] The frequency of occurrence of coronal mass ejections is about an order of magnitude larger at solar maximum than at solar minimum.[26,27] These ejections produce solar wind streams with speeds ranging from several hundred kilometers/second to over 1000

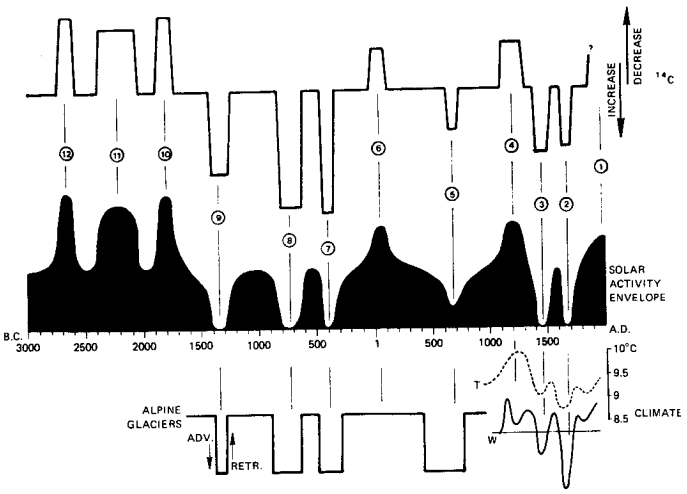

Fig. 5 Interpretation of radiocarbon measurements from tree rings as an indicator of solar activity.[8]

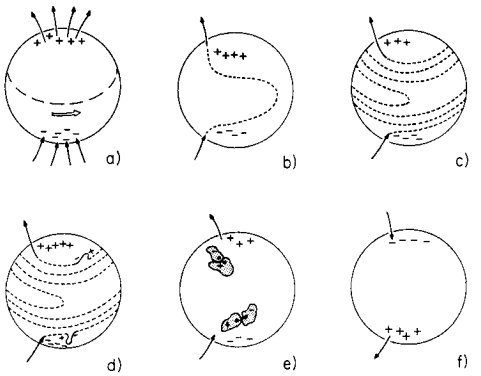

Fig. 6 Babcock's model for the sunspot cycle.[10]

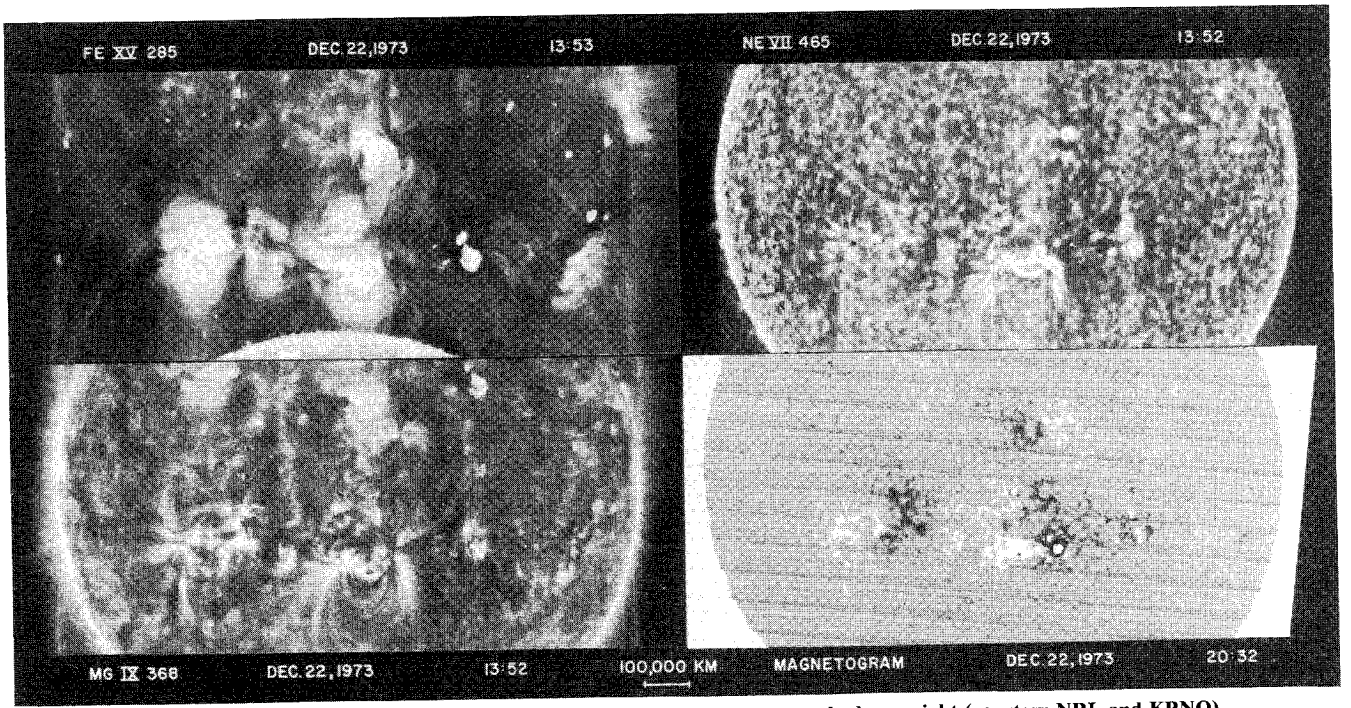

Fig. 7 Skylab EUV spectroheliograms and a Kitt peak magnetogram on the lower right (courtesy NRL and KPNO).

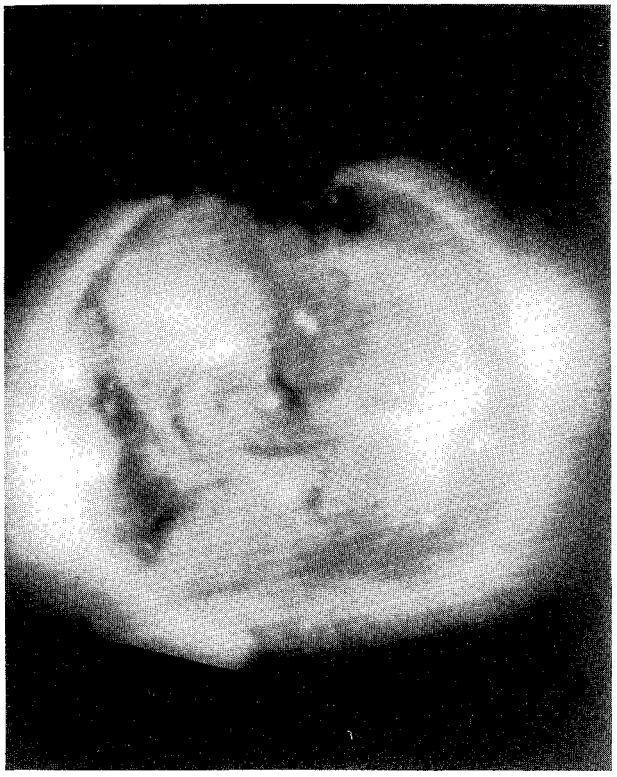

Fig. 8 Skylab x-ray photograph of the sun.

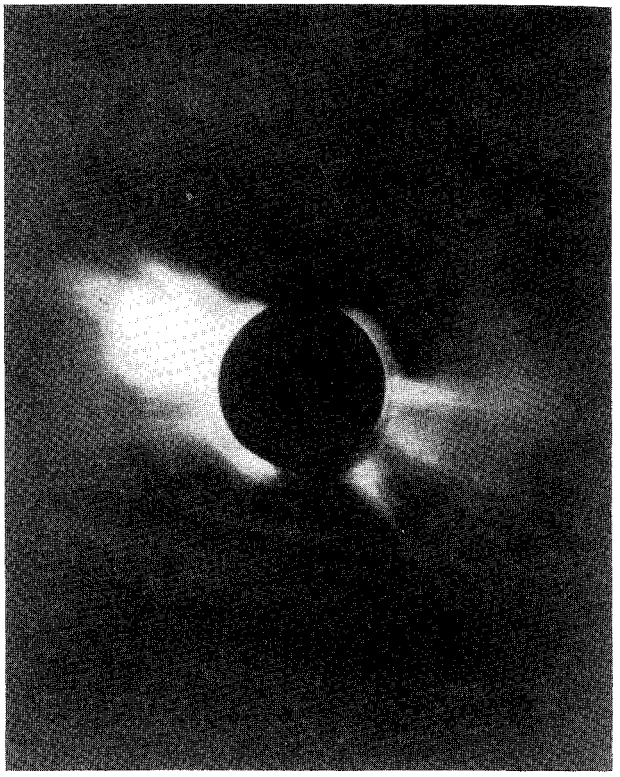

Fig. 9 Large coronal mass ejection.

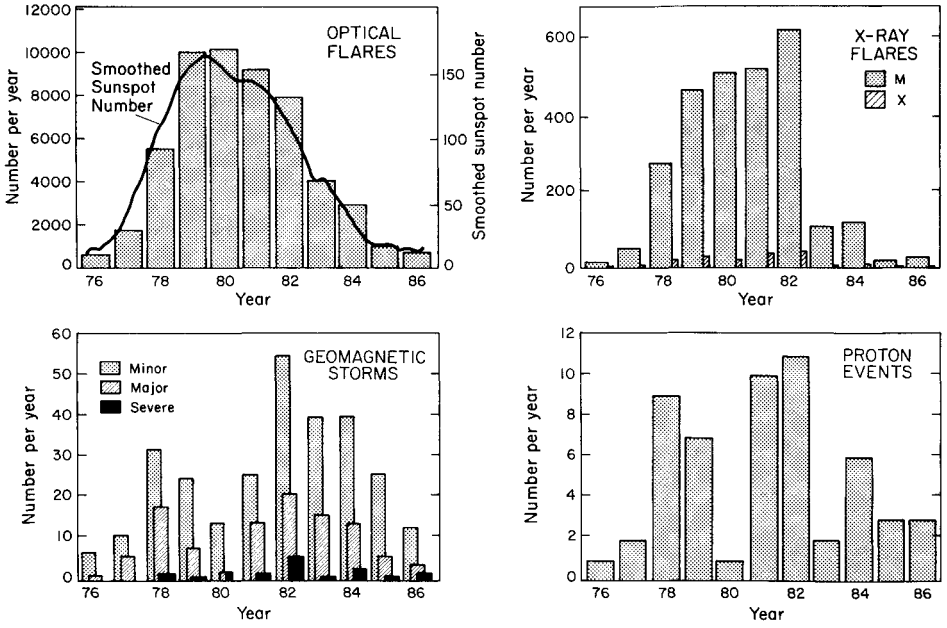

Fig. 10 Solar and geomagnetic activity parameters from cycle 21.[5]

km/s. As mentioned earlier, coronal holes produce high-speed solar wind streams with characteristic speeds of 700 km/s. Because long-lived (months) equatorial coronal holes tend to form at times other than solar maximum, particularly during the declining phase of the solar cycle, they are a major source of recurrent geomagnetic activity then [28] (recurrent because of the 27-day rotation rate of the sun).

Observations of the Current Solar Cycle

The current solar cycle, designated solar cycle 22, has attracted much attention because of its extremely rapid early rise, and because of some predictions that it will have a large to exceptionally large maximum.[5] The rapid rise is significant, because in the past rapid rises in the sunspot number have tended to be associated with larger maxima. Figure 11 shows the early rise of cycle 22 as measured by the smoothed sunspot number and smoothed 10.7-cm radio flux (points).[29] Also plotted as solid lines are the corresponding values for cycles 8–21 (sunspot number) and cycles 19–21 (10.7-cm flux). Cycle 19 had the largest maximum on record. Cycle 22 has been an exceptional cycle thus far, because during its entire early rise phase its solar indices have been equal to or larger than observed in previous cycles. Because of this unprecedented behavior, it is difficult to predict how it will behave in the future. One prediction is shown by the short dash curve (with the long dash cuves defining the 90% prediction interval). We discuss this and other predictions in the following section.

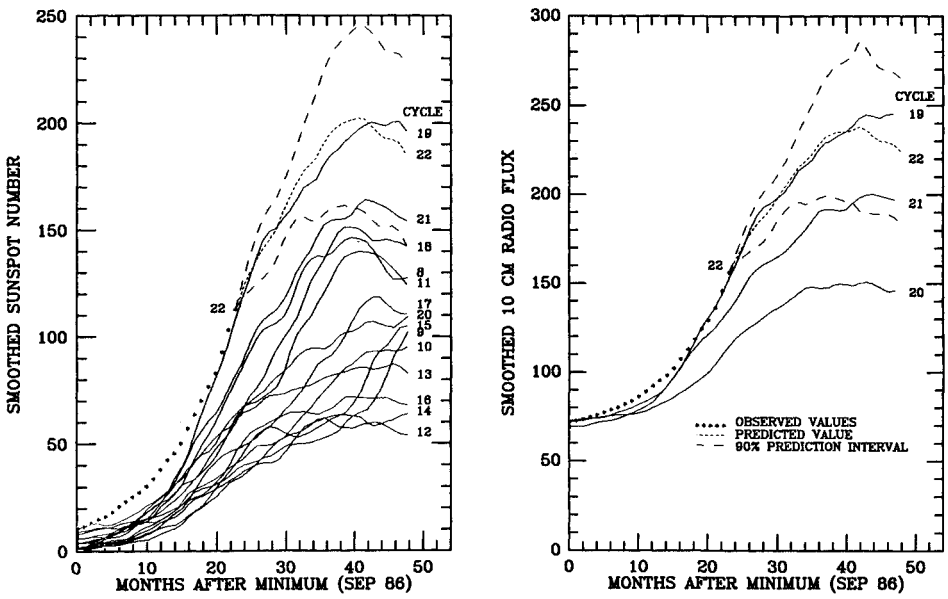

Fig. 11 Rise of cycle 22 compared to earlier cycles (courtesy NOAA Space Environment Lab).[29]

Table 1 Observed[a] percentage of occurrence for maximum spot number $>R_{max}$

R_{max}	$\% > R_{max}$	$\% > R_{max}$ (normal distribution)
200	8	2.1
180	8	6.1
160	17	14.5
140	33	28.1
120	33	46.4
100	58	65.5
80	75	81.1
60	100	91.5

[a]Based on sunspot data from cycles 10-21.[6]

Solar Cycle Predictions

Prediction of future behavior of the sun has practical implications since solar activity affects the terrestrial environment, especially in the regions where spacecraft operate.[24] For example, the schedule for using the Shuttle to reboost the Hubble Space Telescope (HST) to a higher orbit depends on the height of HST's initial orbit and the magnitude of its atmospheric drag, which is very sensitive to solar activity. Scheduling the recovery of spacecraft by the Shuttle also depends on the rate of orbital decay of the spacecraft. A high solar maximum means that orbits of spacecraft such as the long duration exposure facility (LDEF) and the solar maximum mission (SMM) are decaying faster than for a normal cycle.

Prediction of the long-term behavior (months, years) of the solar cycle is difficult because of the its irregularity (e.g., Fig. 2) and due to the lack of a quantitative theory for solar-stellar activity cycles. At the present time, the only way that we can predict the future behavior of the sun is by making use of clues provided by is past behavior. Consider the problem for predicting the magnitude of the sunspot number at the maximum of the current cycle. The basic difficulty is that reliable sunspot numbers exist for only the last 12 cycles. These provide insufficient data to predict unambiguously the future behavior for a phenomenon which is so irregular. Data for many more cycles must be acquired to establish the long-term modulation in the amplitudes of the individual cycles. It is interesting to note that three out of the last four cycles are among the half-dozen largest cycles observed since 1610. Given this, and the rapid rise in the current cycle, we could be experiencing a period when solar activity tends to be higher than normal.

At the present time, there are no reliable long-range methods of predicting solar activity. The difficulty of doing this is illustrated by the wide range of predictions made for the last solar cycle. Figure 12 shows predictions for the magnitude of the sunspot number at solar maximum for cycle 21 varied from 30 to over 200.[30] The observed value was about 160. A zero-order approach to the prediction problem is to assume that all sunspot cycles are independent. Then the probability for having a maximum sunspot number $R \geq R_{max}$ can be estimated from historical data. Table 1 gives the observed percentage of occurrence for the sunspot number at maximum having a value larger than R_{max}. Column 2 gives the observed percentages and the third column gives the percentages expected for values of R_{max} that are normally distributed. The data used for constructing the table are from the 12 most recent sunspot cycles, 10-21. Data prior to 1850 are less reliable.[4] The mean value of R_{max} is 116.4 with a standard deviation of 41.2. If one has no other information, then Table 1 provides an estimate for the probability for the current cycle, cycle 22, having maximum sunspot numbers equal to or larger than a given value.

The zero-order approach ignores other information that is contained in the historical record. In particular, it ignores the fact that there is a correlation between the sunspot numbers at times t_1 and t_2 in a cycle. For example, as mentioned earlier, cycles with rapid rises tend to have larger maxima than average. The zero-order approach also ignores other trends in the historical record, such as the observation than even-numbered cycles tend to have different shapes and lower maxima than odd-numbered cycles. Many authors have used a variety of statistical techniques to determine trends in the sunspot record.[4,6,30,31] For example, there is some evidence for an 80-100-yr modulation.[32] However, given the reliable sunspot numbers are available for only about 140 yr, it is difficult to obtain statistically reliable information about long-term periodicities in the historical record. Proxies for the sunspot number (e.g., auroral observations, ancient naked eye sightings of sunspots, $^{14}C/^{12}C$ ratios in tree rings) can be used to extend the length of the record.[8] However, the uncertainties in these proxies are sufficiently large that they do not provide a reliable basis for predicting future behavior of the solar activity cycle.

Another class of techniques for predicting the magnitude of a solar maximum are the precursor techniques.[30] These techniques are based on the assumption that the behavior of the solar magnetic field in cycle N determines the conditions in cycle $(N+1)$. For example, one may correlate some geomagnetic index during solar minimum (or during the previous solar cycle) with the magnitude of the sunspot number at the following maximum. This makes the additional assumption that there is a casual relationship between the behavior of the specified geomagnetic index and the behavior of the solar magnetic field (which is communicated to the Earth via the solar wind). One can also derive correlations between the solar cyclic behavior of selected solar features in cycle N with the magnitude of the following solar maximum. These correlations and measurements of the behavior of the specified index during the last solar cycle can then be used to estimate the magnitude of the next solar maximum.

Figure 12 illustrates the wide range of predictions made for the maximum sunspot number during the last solar cycle (cycle 21). The solid bars are predictions from statistical methods and the cross-hatched bars are from precursor methods.[30] The observed maximum sunspot number and the $\pm 10\%$ values are plotted as horizontal lines. The precursor methods were more successful than the statistical methods for cycle 21. However, one test does not prove that these methods work. Since there was such a wide range of predictions, spanning nearly the full range of sunspot numbers that have been observed in the past, one would expect some of the techniques to yield the correct value by pure chance.

For relatively short-range predictions (up to about 12 months into the future), the McNish–Lincoln technique[33] is often used. This technique depends on the following assumptions: 1) that to a first approximation, a future value of the sunspot number R at N months after sunspot minimum is the

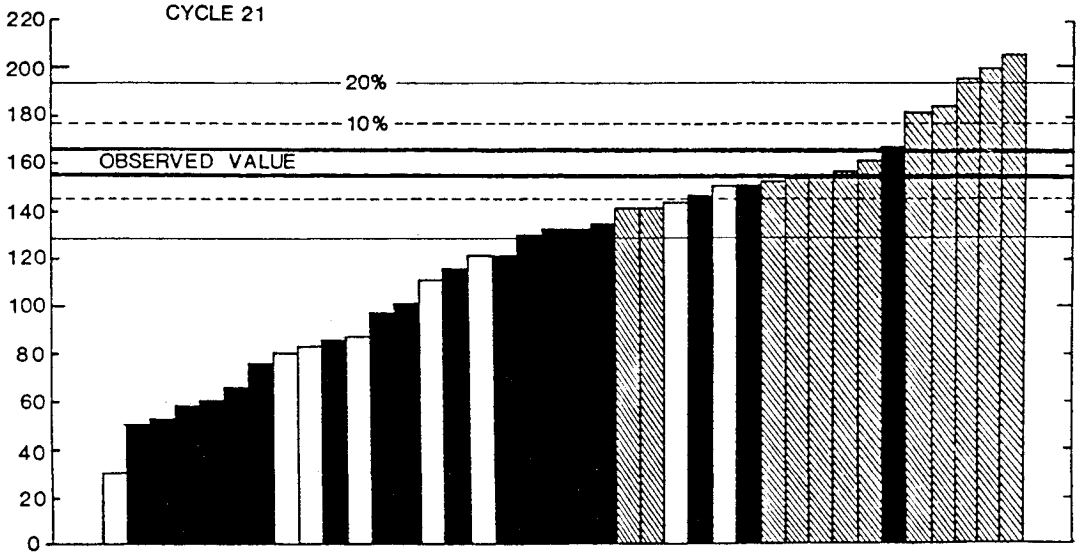

Fig. 12 Predictions for mean sunspot number at maximum of last solar cycle.[30]

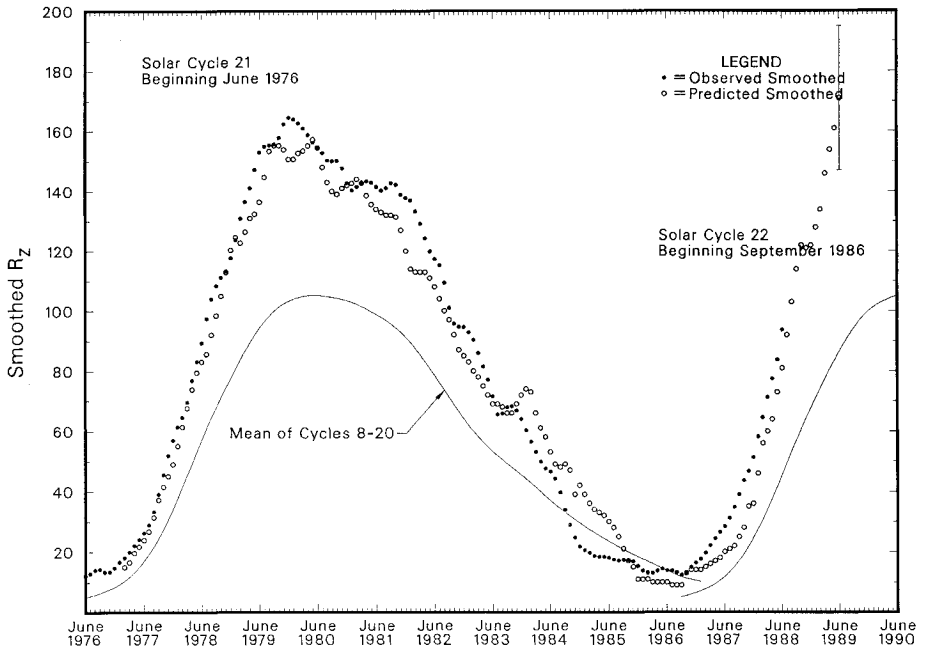

Fig 13. Comparison between predicted and observed sunspot number for past 12 years.[34]

mean $<R(N)>$ from proceeding cycles, and 2) a correction proportional to the sum of the departures $\Delta R(N_i)$ for all months from minimum to month i:

$$R(N) = <R(N)> + k_i \Delta R(N_i) + k_{i-1} \Delta R(N_{i-1}) + \ldots$$

where

$$\Delta R(N_i) = R(N_i) - \langle R(N_i) \rangle$$

Thus, one uses differences between available monthly smoothed sunspot numbers for the current cycle and the corresponding means (determined from earlier cycles) to estimate the difference from the mean of the sunspot number at a future time N months after minimum. This method is intended to give predictions up to about a year beyond the last observation, although it can be used to predict the magnitude of solar maximum. Figure 13 compares the predicted and observed sunspot numbers from the most recent (at the time this review was prepared in January 1989) *Solar-Geophysical Data*.[34] A McNish-Lincoln prediction for the entire cycle is shown in Fig. 11 (dashed curves).[29]

There are a wide range of predicted values for the maximum sunspot number in cycle 22, ranging from less than 40–200 (see Table 2 and Brown and Simon[30]). Table 2 summarizes a number of predictions. For the precursor techniques, we have used primarily recent values. For the statistical techniques, we give the mean of the values quoted by Brown and Simon[30] and several more recent results. Based on the data available in early 1989, it appears that the values in Table 2 that are based on statistical techniques (other than McNish-Lincoln) will underestimate the magnitude of cycle 22. As mentioned earlier, the statistical techniques also underestimated the magnitude of cycle 21. The values predicted for cycle 22 by the precursor techniques still appear to be viable. Taken as a group with equal weighting they yield an estimate for the mean sunspot number at maximum of 154 ± 45 (2σ). Since the uncertainties in the McNish-Lincoln prediction decrease with decreasing time between the time of the last sunspot data and the time of maximum, it ultimately will provide the most reliable prediction. The January-February 1989 NOAA predictions with the McNish-Lincoln technique (Table 2) yield $R_{max} = 198 \pm 52$ with maximum occurring in about February 1990. Taken together, the precursor and McNish-Lincoln predictions, along with the rapid rise of cycle 22, indicate that this cycle will have moderate to high levels of activity. There is a finite probability, as large as 10–20% or more, that cycle 22 may be exceptional and have a sunspot maximum larger than that in 1957–1958 during cycle 19, which had the largest sunspot maximum on record. Evidence for this is the rapid rise in cycle 22, the high levels of activity in December and January (only 5 months in cycle 19 had 10-cm fluxes larger than the January 1989 value, P. McIntosh, private communication), and the current McNish-Lincoln predictions, which predict near record levels (and whose uncertainty limits include the possibility of larger or smaller levels; see Fig. 11).

A final note of caution: It must be emphasized that all of the proceeding predictions depend in some way on correlations between some parameter (or set of parameters) and the magnitude of solar maximum. Apparently good correlations between two phenomena do not necessarily prove that the phenomena are causally connected.

Table 2 Predictions for solar cycle 22 (smoothed sunspot number)

Author	Reference	Technique	Cycle 22 prediciton	Error, 2σ
Brown	35	Precursor	174	35
Brown	35	Precursor	175	35
Kane	36	Precursor	165	35
Lantos and Simon	37	Precursor	110	40
Sargent	38	Precursor	119	50
Schatten and Sofia	40	Precursor	170	50
Thompson	41	Precursor	163	none
Wilson	42	Precursor	145	8
Wilson	43	Precursor	154	70
Wilson	43	Precursor	164	40
Lindberg	44	McNish-Lincoln	179	—
NOAA/NESDIS	34	McNish-Lincoln	192	51
NOAA/SEL	45	McNish-Lincoln	203	52
Brown and Simon	30	Statistical	100	45
Wilson	6	Statistical	107	73
Wilson	46	Statistical	75	49

Summary and Conclusions

The solar output of short-wavelength radiation, solar wind, and energetic particles depends strongly on the solar magnetic cycle. Because of the effects of these outputs on the interplanetary and terrestrial environments, it is desirable to predict the future behavior of the magnetic cycle. However, this is difficult due to the lack of a suitable quantitative theory for this cycle, its irregularity, and the small number of cycles for which reliable measurements of relevant solar indices exist. In spite of these limitations, there are indications that the current cycle will have moderate to exceptionally high levels of activity. These indications are based on 1) the exceptionally rapid rise of cycle 22 in the past 2 yr (and the correlation between rapid rise rates and high maxima in the past cycles) and 2) the behavior of solar or geomagnetic phenomena during the decay of cycle 21 (and the correlation between these phenomena and the magnitude of subsequent solar maxima in past cycles). Given these results, we can expect that during the next few years the solar flux of short-wavelength radiation and particles will be more intense than normal, and the spacecraft in low Earth orbit will re-enter earlier than usual.

Acknowledgments

I would like to express my appreciation to S. Greer, G. R. Heckman, E. Hildner, J. W. Hirman, P. S. McIntosh, H. H. Sargent, J. B. Smith Jr., and R. M. Wilson for helpful and informative comments, advice, and material on the subject of this paper.

References

[1]Lean, J., "Solar Ultraviolet Irradiance Variations: A Review," *Journal of Geophysical Research,* Vol. 92, Jan. 1987, pp. 839-868.

[2]Schwabe, H., "Solar Observations during 1843," *Astronomische Nacrichten,* Vol. 21, Dec. 1843, pp. 233-236; also, *Early Solar Physics,* edited by A. J. Meadows, Pergamon, London, 1970, p. 312.

[3]Bray, R. J. and Loughhead, R. E., *Sunspots,* Chapman and Hall, London, 1964, p. 237.

[4]Eddy J. A., "Historical Evidence for the Existence of the Solar Cycle," *The Solar Output and its Variation,* edited by O. R. White, Colorado Assoc. Univ. Press, Boulder, CO, 1977, pp. 51-72.

[5]Hirman, J. W., Heckman, G. R., Greer, M. S., and Smith, J. B., "Solar and Geomagnetic Activity during Cycle 21 and Implications for Cycle 22," *EOS, Transactions, American Geophysical Union,* Vol. 69, Oct. 1988, pp. 962-973.

[6]Wilson, R. M., "A Comparative Look at Sunspot Cycles," NASA 2325, May 1984.

[7]Hedin, A. E. and Mayr, H. G., "Solar EUV-Induced Variation in the Thermosphere," *Journal of Geophysical Research,* Vol. 92, Jan. 1987, pp. 869–875.

[8]Eddy, J. A., "Historical and Arboreal Evidence for a Changing Sun," *The New Solar Physics,* edited by J. A. Eddy, AAAS Selected Symposium 17, Westview Press, Boulder, CO, 1978, pp. 11–33.

[9]Babcock, H. W., "The Topology of the Sun's Magnetic Field and the 22-Year Cycle," *Astrophysical Journal,* Vol. 133, March 1961, pp. 572–587.

[10]Noyes, R. W., *The Sun, Our Star,* Harvard Univ. Press, Cambridge, MA, 1982, pp. 111–114.

[11]Hundhausen, A. J., *Coronal Expansion and the Solar Wind,* Springer-Verlag, New York, 1972, pp. 1–238.

[12]Axford, W. I., "The Solar Winds," *Solar Physics,* Vol. 100, 1985, pp. 575–586.

[13]Pizzo, V. J., Holzer, T. E., and Sime, D. G. (eds.), *Proceedings of the Sixth International Solar Wind Conference,* National Center for Atmospheric Research, Boulder, CO, NCAR/TN-306+Proc, 1988, pp. 1–714.

[14]Krieger, A. S., Timothy, A. F., and Roelof, E. C., "A Coronal Hole as the Source of a High-Velocity Solar Wind Stream," *Solar Physics,* Vol. 29, 1973, pp. 505–525.

[15]Feldman, W. C., Asbridge, J. R., Bame, S. J., and Gosling, J. T., "Plasma and Magneic Fields from the Sun," *Solar Output and Its Variations,* edited by O. R. White, Colorado Assoc. Univ. Press, Boulder, CO, 1977, pp. 351–328.

[16]Zirker, J. B., *Coronal Holes and High-Speed Solar Wind Streams,* Colorado Assoc. Univ. Press, Boulder, CO, 1977, pp. 1–454.

[17]Schwenn, R., "The 'Average' Soalr Wind in the Inner Heliosphere: Structures and Slow Variations," *Solar Wind Five,* edited by M. Neugebauer, NASA, Washington DC, 1983, pp. 489–507.

[18]Withbroe, G. L., "Origins of the Solar Wind in the Corona," *The Sun and the Heliosphere in Three Dimensions,* edied by R. G. Marsden, Reidel, Dordrecht, Holland, 1986, pp. 19–32.

[19]Sturrock, P. A. (ed.), *Solar Flares,* Colorado Assoc. Univ. Press, Boulder, CO, 1980, pp. 1–513.

[20]Kundu, M. and Woodgate, B. (eds.), *Energetic Phenomena on the Sun,* NASA 2439, NASA, Washington D.C., 1986, pp. 1–426.

[21]Dennis, B. R., Orwig, L. E., and Kiplinger, A. L. (eds.), *Rapid Fluctuations in Solar Flares,* NASA 2449, NASA, Washington DC, 1987, pp. 1–478.

[22]Wagner, W. J., "Coronal Mass Ejections," *Annual Review of Astronomy and Astrophysics,* Vol. 22, 1984, pp. 267–289.

[23]Hundhausen, A. J., "The Origin and Propagation of Coronal Mass Ejections," *Proceedings of the Sixth International Solar Wind Conference,* edited by V. J. Pizzo, T. E. Holzer, and D. G. Sime, NCAR, Boulder, CO, NCAR/TN-306+Proc, 1988, pp. 181–214.

[24]Gorney, D. J., "Solar Cycle Effects on Near-Earth Plasmas and Space Systems," *Journal of Spacecraft and Rockets,* Vol. 26, 1989.

[25]Hewish, A., "The Solar Origin of Geomagnetic Storms," *Solar Physics,* Vol. 116, 1987, pp. 195–198.

[26]Kahler, S., "Observations of Coronal Mass Ejections near the Sun," *Proceedings of the Sixth International Solar Wind Conference,* edited by V. J. Pizzo, T. E. Holzer, and D. G. Sime, National Center for Atmospheric Research, Boulder, CO, NCAR/TN-306+Proc, 1988, pp. 215–231.

[27]Feynman, J. and Garrett, H. B., "Solar Cycle Dependence of Major Equatorial Coronal Mass Ejections Rate (from proxy data)," *Proceedings of the Sixth International Solar Wind Conference,* edited by V. J. Pizzo, T. E. Holzer, and D. G. Sime, National Center of Atmospheric Research, Boulder, CO, NCAR/TN-306+Proc, 1988, pp. 279–285.

[28]Sheeley, N. R., Jr. and Harvey, J., "Coronal Holes, Solar Wind Streams, and Geomagnetic Disurbances during 1978 and 1979," *Solar Physics,* Vol. 70, 1981, pp. 237–249.

[29]Solar-Geophysial Data 1989, *Preliminary Report and Forecast of Solar-Geophysical Data,* SESC PRF 702, National Oceanic and Atmpspheric Administration, Space Environmental Research Lab., Boulder, CO.

[30]Brown, G. M. and Simon, P. A., "Long-Term Solar Activity Predictions," *Solar-Terrestrial Predictions: Proceedings of a Workshop at Meudon, France June 18–22, 1984,* edited by P. Simon, G. Heckman, M. A. Shea, NOAA, Boulder, CO, 1986, pp. 1–7.

[31]Simon, P. A., Heckman, G., and Shea, M. A. (eds.), *Solar-Terrestrial Predictions: Proceedings of a Workshop at Meudon, France June 18–22, 1984,* National Oceanic and Atmospheric Administration, Boulder, CO, 1986, pp. 1–632.

[32]Gleissberg, W., "The Eighty-Year Sunspot Cycle," *Journal of the British Astronomical Association,* Vol. 68, Jan. 29, 1958, pp. 148–152.

[33]McNish, A. G. and Lincoln, J. V., "Predictions of Sunspot Numbers," *EOS, Transactions, American Geophysical Union,* Vol. 30, Oct. 1949, pp. 673–685.

[34]Solar-Geophysical Data 1989, *Solar-Geophysical Data Prompt Reports,* Jan. 1989, No. 533, National Oceanic and Atmospheric Administration, National Environmental Satellite, Data, and Information Service, NOAA, Boulder, CO.

[35]Brown, G. M., "Solar Cycle 22 to be One of the Largest on Record?," *Nature*, Vol. 333, May 12, 1988, pp. 121, 122.

[36]Kane, R. P., "Prediction of the Maximum Annual Mean Sunspot Number in the Coming Solar Maximum Epoch," *Solar Physics,* Vol. 108, 1987, pp. 415, 416.

[37]Lantos, P. and Simon, P., "Prediction of the Next Solar Activity Cycle," *Proceedings of the 8th ESA Symposium on European Rocket and Ballooon Programes and Related Research,* European Space Agency, Noordwijk, SP-270, 1987, pp. 451–453.

[38]Sargent, H. H., III, "A Prediction for the Next Sunspot Cycle," *Proceedings of the 28th IEEE Vechicular Technical Conference,* Denver, 1978, pp. 490–496; also see Ref. 39.

[39]"Solar-Geophysial Data Sept. 1987," *Preliminary Report and Forecast of Solar-Geophysical Data,* National Oceanic and Atmpspheric Administration, Space Environmental Research Lab., Boulder, CO, SESC PRF 626.

[40]Schatten, K. H. and Sofia, S., "Forecast of an Exceptionally Large Even-Numbered Solar Cycle," *Geophysical Research Letters,* Vol. 14, 1987, pp. 632–635.

[41]Thompson, R. J., "Solar-Geophysical Data Sept. 1987," *Preliminary Report and Forecast of Solar-Geophysical Data,* National Oceanic and Atmospheric Administration, Space Environment Research Lab., Boulder, CO, SESC PRF 626, p. 12.

[42]Wilson, R. M., "An Alternative View of the Size of Solar Cycle 22," *Nature,* Vol. 335, Oct. 27, 1988, p. 773.

[43]Wilson, R. M., "A Prediction for the Maximum Phase and Duration of Sunspot Cycle 22," *Journal of Geophysical Research,* Vol. 93, Sept. 1988, pp. 10011–10015.

[44]Lindberg, J. P., "Solar Activity Inputs for Upper Atmospheric Models Used in Programs to Estimate Spacecraft Orbital Lifetime," NASA Marshall Space Flight Center, private communication, 1989.

[45]Hirman, J., NOAA Space Environment Lab., private communciation, 1989.

[46]Wilson, R. M., "On the Long-Term Secular Increase in Sunspot Number," Solar Physics, Vol. 115, 1988, pp. 397–408.